

¹ Estimating the fitness cost and benefit of antimicrobial resistance from
² pathogen genomic data

³ David Helekal¹, Matt Keeling², Yonatan H Grad³, Xavier Didelot^{4,*}

⁴ ¹ Centre for Doctoral Training in Mathematics for Real-World Systems, University of Warwick, UK

⁵ ² Mathematics Institute and School of Life Sciences, University of Warwick, UK

⁶ ³ Department of Immunology and Infectious Diseases, TH Chan School of Public Health, Harvard
⁷ University, USA

⁸ ⁴ School of Life Sciences and Department of Statistics, University of Warwick, UK

⁹ ^{*} Corresponding author. Tel: 0044 (0)2476 572827. Email: xavier.didelot@warwick.ac.uk

¹⁴ Running title: Phylodynamics of pathogen antimicrobial resistance

¹⁵ ¹⁶ Keywords: genomic epidemiology, phylodynamics, antimicrobial resistance, resistance fitness cost

17 ABSTRACT

18 Increasing levels of antibiotic resistance in many bacterial pathogen populations is a major threat
19 to public health. Resistance to an antibiotic provides a fitness benefit when the bacteria is exposed
20 to this antibiotic, but resistance also often comes at a cost to the resistant pathogen relative to
21 susceptible counterparts. We lack a good understanding of these benefits and costs of resistance for
22 many bacterial pathogens and antibiotics, but estimating them could lead to better use of antibiotics
23 in a way that reduces or prevents the spread of resistance. Here, we propose a new model for the
24 joint epidemiology of susceptible and resistant variants, which includes explicit parameters for the cost
25 and benefit of resistance. We show how Bayesian inference can be performed under this model using
26 phylogenetic data from susceptible and resistant lineages and that by combining data from both we are
27 able to disentangle and estimate the resistance cost and benefit parameters separately. We applied our
28 inferential methodology to several simulated datasets to demonstrate good scalability and accuracy.
29 We analysed a dataset of *Neisseria gonorrhoeae* genomes collected between 2000 and 2013 in the USA.
30 We found that two unrelated lineages resistant to fluoroquinolones shared similar epidemic dynamics
31 and resistance parameters. Fluoroquinolones were abandoned for the treatment of gonorrhoea due to
32 increasing levels of resistance, but our results suggest that they could be used to treat a minority of
33 around 10% of cases without causing resistance to grow again.

34 INTRODUCTION

35 The levels of antimicrobial resistance of many pathogens have risen worryingly over the past few
36 decades. In a report on the threat posed by antibiotic resistance published by the CDC (Centres
37 for Disease Control and Protection), three microorganisms including *N. gonorrhoeae* are classified as
38 posing an urgent threat level, and twelve more represent a serious threat to public health [1]. A
39 review on antimicrobial resistance estimated that resistance claims at least 700,000 lives per year
40 worldwide and that the death toll could go up to 10 million per year by 2050 if current trends
41 are allowed to continue [2], and a recent study estimated that there were almost 5 million deaths
42 associated with resistance in 2019 [3]. Few new antimicrobials have been developed and deployed
43 since the 1970s, whereas resistance to new drugs often emerges soon after initial introduction [4],
44 so that several pathogens are dangerously close to becoming completely untreatable. Effectively
45 tackling antimicrobial resistance requires greater understanding of epidemiological and evolutionary
46 factors leading to emergence of resistance and the spread of resistance through pathogen populations.
47 Achieving this goal requires development of mathematical models of antimicrobial resistance and robust
48 statistical analysis of epidemiological models with informative observations. This modelling approach
49 to resistance was initiated in the late 1990s [5, 6] and has led to the development of many models,
50 appropriate for different organisms, mode of spread, study scale and context [7].

51 Resistance brings a clear fitness benefit to pathogens acquiring it in the presence of antimicrobials.
52 The net value of this fitness benefit therefore increases with the frequency with which the specific
53 antimicrobial is employed, either against the pathogen itself or more generally in the case of a pathogen
54 that can be carried asymptotically. However, resistance also typically comes with a fitness cost to the
55 pathogen [8]. The simplest demonstration of this effect is when discontinued use of an antimicrobial
56 leads to reductions in resistance rates. The fitness costs and benefits of resistance remain poorly
57 understood for many pathogens and antimicrobials [9]. A better quantification of resistance benefits
58 and costs is required to provide a solid basis for evaluating the potential effectiveness of public health
59 intervention measures proposed to exploit fitness costs in the hope of stopping or even reversing the
60 spread of resistance [9]. For example, the numbers of gonorrhoea cases sensitive and resistant to
61 cefixime in England over a decade was recently analysed to quantify the cost and benefit associated
62 with resistance to this antibiotic [10]. These estimates were used to predict that cefixime could
63 be reintroduced to treat a minority ($\sim 25\%$) of gonorrhoea cases without causing an increase in
64 cefixime resistance levels, which would reduce the risk of emergence of resistance to the currently used
65 antibiotics. Moreover, the extent of the fitness cost of resistance can vary by genomic background [11],
66 such that the effect of interventions that seek to capitalize on the fitness costs of resistance may be
67 lineage dependent. Therefore, it is necessary to estimate fitness costs at the per lineage level. The aim
68 of this study is to quantify the contribution that changes in prescription policy have on the population
69 dynamics of particular resistant lineages. This is in contrast to studies that are interested in the overall
70 ecology of resistance or the eventual fate of a resistant phenotypes, see for example [12].

71 Pathogen genomic data has great potential to help us understand the evolutionary and epidemiological
72 dynamics of infectious disease [13]. An important advantage of this phylodynamic approach is that
73 analysis of genomic data is less sensitive to sampling biases, especially when using a coalescent
74 framework which describes the ancestry process conditional on sampling [14]. A few studies have used
75 this approach to shed light on the fitness cost associated with antimicrobial resistance. For example, a
76 study showed the association between the growth rate of a methicillin-resistant *Staphylococcus aureus*
77 lineage and consumption of beta-lactams [15]. Other studies quantified the relative transmission fitness
78 of resistance mutations in HIV [16] and *Mycobacterium tuberculosis* [17]. Here, we take a different
79 approach by modelling explicitly the phylodynamic trajectories of the sensitive and resistant lineages
80 as a function of the fitness cost, which is constant, and the fitness benefit, which depends on the

81 antimicrobial consumption. Our method therefore requires three inputs: the amount of antimicrobial
82 being used over time, genomic data from a sensitive lineage, and genomic data from a resistant lineage.
83 From this we disentangle the fitness cost and benefit of resistance, thereby providing the parameters
84 needed to predict phylodynamic trajectories and inform recommendations on how to use antimicrobials
85 without worsening the resistance threat. Overall, the scenario we are interested in is that of overall
86 resistance dynamics at a large population level. In such a scenario the bulk of incidence is going to be
87 caused by local transmission rather than imports. We do not intend for the methods presented in this
88 paper to be applicable to small population dominated by imports and complex, heterogeneous routes
89 of transmission, such as within hospital setting of hospital acquired infections. For such a scenario, a
90 different approach using Birth-Death type models would be more appropriate [16, 17].

91 METHODS

92 Overall approach

93 Pathogen phylogenetic data contains information about past population size dynamics of the pathogen
94 under study [13, 18]. Under assumptions of the epidemic process being characterised well enough by
95 a simple compartmental epidemic model, this information about population size dynamics can be
96 translated into epidemic trajectories [19, 20]. These epidemic trajectories can be described using an
97 epidemic model which accounts for the effects of a fitness cost and benefit of resistance to a specific
98 antimicrobial. As the use of this antimicrobial changes through time, so will the net fitness of the
99 particular lineage in consideration. This will in turn lead to changes in the behaviour of the epidemic
100 trajectory. However, not all changes in the behaviour of the epidemic trajectory will be due to changes
101 in the fitness of the resistant phenotype. Confounding factors, such as as depletion of susceptibles or
102 changes in host behaviour will also affect the epidemic trajectory. Under relatively mild assumptions
103 detailed below changes in these confounding factors will affect other lineages equally. We can therefore
104 use as “control” some data from a susceptible lineage, ideally closely related and with the same
105 resistance profile to other antimicrobials used in significant amounts as primary treatment. Differences
106 between the trajectories of the sensitive and resistant lineages can then be ascribed specifically to
107 resistance, allowing us to estimate the associated fitness cost and benefit parameters.

108 Let us consider a pathogen causing infections at the level of a large population that are or were
109 treated with a certain antimicrobial compound. We assume that at some point in the past one or
110 several lineages with resistance to this antimicrobial compound have arisen. Our aim is to quantify
111 the fitness cost and benefit of the resistance to this antimicrobial for a given lineage as a function of
112 use of the antimicrobial of interest through time. To this end we need data that quantify the use over
113 time of the given antimicrobial to treat infections caused by this pathogen, as well as a reasonable
114 sample of sequenced case isolates from infections caused by the pathogen over time. Furthermore,
115 we need information that characterises the resistance profiles of the individual isolates, which can be
116 obtained either by resistance screening *in vitro*, or predicted from the sequences *in silico* [21]. A dated
117 phylogeny of these samples is estimated, for example using BEAST [22], BEAST2 [23] or BactDating
118 [24]. This phylogeny is then used as the starting point for analysis [25], to identify which samples
119 belong to resistant and susceptible lineages and to select related lineages for further study that are
120 wholly resistant or susceptible to the antimicrobial of interest, but otherwise similar in their resistance
121 profiles. Note that for simplicity resistance is treated as a binary trait, with samples being either
122 resistant or susceptible to antimicrobials, as is usually the case in resistance modelling studies [7].

123 **Transmission model derivation**

124 In order to estimate the fitness cost and benefit of antimicrobial resistance, a transmission model
 125 needs to be specified. We focus on estimating the fitness parameters of a particular lineage harbouring
 126 a certain treatment resistant phenotype when previous infection does not confer immunity against
 127 reinfection. Under the simplifying assumptions that the host population is unstructured and that past
 128 infections do not confer any immunity, the multi-lineage Susceptible-Infected-Susceptible (SIS) is a
 129 reasonable model [26, 27]. This model is more commonly referred to as multi-strain SIS. Fluctuations
 130 in the carriage levels of different lineages can also be due to external factors, such as changes in host
 131 demography or behaviours. Left unaccounted, such fluctuations would bias estimates of the fitness cost
 132 and benefit of resistance to a given antimicrobial. Therefore, we modify the model with time-varying
 133 transmission rate $\beta(t)$ and population size $N(t)$. This leads to an n -lineage model described by a
 134 system of the following n -coupled ordinary differential equations (ODEs):

$$\begin{aligned} \frac{dI_1(t)}{dt} &= \frac{\beta(t)S(t)I_1(t)}{N(t)} - \gamma_1(t)I_1(t) \\ \frac{dI_2(t)}{dt} &= \frac{\beta(t)S(t)I_2(t)}{N(t)} - \gamma_2(t)I_2(t) \\ &\vdots \\ \frac{dI_n(t)}{dt} &= \frac{\beta(t)S(t)I_n(t)}{N(t)} - \gamma_n(t)I_n(t) \end{aligned} \quad (1)$$

135 Where $I_j(t)$ denotes the number of people infected with the j -th lineage at time t . $\beta(t)$ is the
 136 transmission rate that varies with time due for example to changes that are not specific to any lineage,
 137 for example host behaviour. $N(t)$ is the host population size which may also change with time due to
 138 demographic factors. $\gamma_j(t)$ is the recovery rate of the j -th lineage at time t . These may or may not
 139 vary with time through their dependency on the antimicrobial usage which changes with time. Finally
 140 $S(t)$ denotes the number of susceptible hosts

$$S(t) = \left(N(t) - \sum_{j=1}^n I_j(t) \right) \quad (2)$$

141 Typically this model could simply be reduced to a two lineage model, averaging over all lineages
 142 that are phenotypically similar in their resistance profiles. However, this is undesirable, as some of the
 143 lineages with the same resistance phenotype could differ in fitness due to different genomic background
 144 which would confound our estimates. Furthermore this sort of model would not be readily tractable
 145 in a genomic framework, because phylogenetic data is generally going to be informative about the
 146 dynamics of a particular lineage only. Note that this also means that the analysis produced is valid
 147 for the lineages being studied, and cannot be extrapolated to the overall dynamics of resistance for a
 148 given pathogen.

149 We therefore need to focus on the resolution of individual lineages. We note that environmental effects
 150 such as fluctuations in host population size or behaviour affect all lineages equally, if the population
 151 is well mixed. We denote the combination of these effects as $b(t) = \beta(t)S(t)/N(t)$. Conditional on the
 152 knowledge trajectory of $b(t)$ the ODEs in Equation 1 become uncoupled, and this allows us to reduce
 153 the system to uncoupled equations corresponding to the lineage we will be focusing on. As such we
 154 will treat $b(t)$ as a random object that needs to be inferred. We further assume that for the susceptible
 155 lineages the average recovery rate denoted γ_s does not change over time, whereas for the resistant
 156 lineage it takes one of two values: $\gamma_T = q_T + \gamma_s$ if a given patient is treated with the antimicrobial
 157 of interest, or $\gamma_U = q_U + \gamma_s$ otherwise. If we also consider the known proportion of registered cases

158 treated with the antimicrobial of interest $u(t)$, this fully determines the average recovery rate of the
 159 resistant lineages as:

$$\gamma_r(t) = u(t)\gamma_T + (1 - u(t))\gamma_U \quad (3)$$

160 We can now fully write down the equations of the model we will be using for the sensitive and resistant
 161 lineages, respectively:

$$\begin{aligned} \frac{dI_s(t)}{dt} &= b(t)I_s(t) - \gamma_s I_s(t) \\ \frac{dI_r(t)}{dt} &= b(t)I_r(t) - [u(t)\gamma_T + (1 - u(t))\gamma_U] I_r(t) \end{aligned} \quad (4)$$

162 In practice, we are interested in the difference in recovery rates between the susceptible and the resistant
 163 lineage and sensitive lineage when every case gets treated with the antimicrobial of interest, and when
 164 the antimicrobial of interest is not used at all. We denote these by

$$\begin{aligned} q_T &= \gamma_T - \gamma_s \\ q_U &= \gamma_U - \gamma_s \end{aligned} \quad (5)$$

165 The interpretation is therefore that q_T captures the fitness benefit of resistance in the case $q_T < 0$ and
 166 q_U captures the fitness cost of resistance in the case $q_U > 0$.

167 This model can be applied to any number of resistant and sensitive lineages, simply by adding lineages
 168 associated terms to the likelihood and adding required parameters. This is straightforward as the
 169 individual lineages are independent conditional on $b(t)$. but for simplicity the remainder of methods
 170 description focuses on the case of a single sensitive and a single resistant lineage, with the general case
 171 being a straightforward extension.

172 Link to phylogenies

173 Having defined the epidemiological model, we can now link it to the phylogenetic process. Based on
 174 [19, 28], the instantaneous coalescent rates for a single pair of lineages can be derived as

$$\lambda_s(t) = \frac{2b(t)}{I_s(t)} \text{ and } \lambda_r(t) = \frac{2b(t)}{I_r(t)} \quad (6)$$

175 in the susceptible and resistant populations, respectively. The likelihood of a dated phylogeny \mathbf{g} with
 176 n leaves at times $s_1 < \dots < s_n$ and $n - 1$ coalescent events at times $c_1 < \dots < c_{n-1}$ and $A(t)$ lineages
 177 at time t is therefore given by [29]:

$$p(\mathbf{g}|\lambda(t)) = \exp \left(- \int_{-\infty}^{\infty} \mathbb{1}[A(t) \geq 2] \binom{A(t)}{2} \lambda(t) dt \right) \prod_{i=1}^{n-1} \lambda(c_i) \quad (7)$$

178 Where $\lambda(t) = \lambda_s(t)$ and $\lambda(t) = \lambda_r(t)$ for the susceptible and resistant phylogenies, respectively.
 179 However, in most cases, and indeed in our case, the integral in Equation 7 is not analytically intractable.
 180 Furthermore, the antibiotic use data is unlikely to span the entire phylogeny. Therefore, we define the
 181 approximate likelihood for the phylogeny truncated to $[t_{\min}, t_{\max}]$, which is the intersection interval
 182 spanned by the antibiotic use data and the phylogenies under study.

183 As such we resort to the standard way of approximating coalescent likelihoods [30], partitioning the
 184 interval $[t_{\min}, t_{\max}]$ into a fine mesh $t_{\min} = t_1 < t_2 < t_3 < \dots < t_N = t_{\max}$ such that $t_i - t_{i-1} < \Delta_t$ and
 185 that all sampling and coalescent times between t_{\min} and t_{\max} are included in the mesh:

$$p(\mathbf{g}|\lambda(t)) = \exp \left(- \sum_{i=2}^N (t_i - t_{i-1}) \binom{A(t_{i-1})}{2} \lambda(t_{i-1}) \right) \prod_{i=1}^{n-1} \mathbb{1}[c_i \in [t_{\min}, t_{\max}]] \lambda(c_i) \quad (8)$$

186 We note that the approach of how we treat the relationship between the phylogenies and epidemic
 187 is effectively a structured coalescent with no migration and time varying $N_e(t)$ determined by the
 188 deterministic epidemic model. Approaches reminiscent of ours have been used to formally study the
 189 expected age of a mutation in both presence or absence of selection [31]. However in that case the
 190 populations correspond to different alleles, and the $N_e(t)$ curves follow the proportion of population
 191 with a given allele as determined by Wright-Fisher diffusion forwards in time. Migration between the
 192 demes corresponding to individual alleles can also further be added corresponding to recombination
 193 [32].

194 Bayesian inference

195 We first re-scale time from the interval $[t_{\min}, t_{\max}]$ to $[-1, 1]$. Denoting the scale factor $D =$
 196 $(t_{\max} - t_{\min})/2$ associated with this re-scaling, we account for this in the model by defining $\bar{\gamma}_s = \gamma_s D$.
 197 The model consists of independent first-order linear homogeneous ODEs for each lineage with time-
 198 varying coefficients. The solutions at time t subject to initial conditions $I_s(0) = I_{s0}$ and $I_r(0) = I_{r0}$
 199 can be obtained in terms of the integral of the instantaneous rates up to time t :

$$\begin{aligned} I_s(t) &= I_{s0} \exp \left\{ \int_0^t b(\tau) - \gamma_s d\tau \right\} \\ I_r(t) &= I_{r0} \exp \left\{ \int_0^t b(\tau) - [u(\tau)\gamma_T + (1 - u(\tau))\gamma_U] d\tau \right\} \end{aligned} \quad (9)$$

200 As it stands, this model would not be well-suited for performing inference under, primarily due to the
 201 difficulty in choosing a sensible prior on $b(t)$, and a very complicated dependency structure between the
 202 initial conditions and $b(t)$. As such we re-parameterise the model by directly modelling the logarithm
 203 of $I_s(t)$ as a Gaussian Process:

$$C(t) = \log I_s(t) - \mu_s \quad (10)$$

204 Where $C(t)$ is an appropriately chosen zero mean Gaussian Process, and μ_s is the susceptible intercept
 205 which relates to the susceptible initial condition I_{s0} as follows:

$$\mu_s = \log I_{s0} - C(0) \quad (11)$$

206 We use this formulation principally to loosen the coupling between the intercept parameter and the
 207 Gaussian Process in order to speed up sampling. From this we can compute $b(t)$ and $\log I_r(t)$ as

$$b(t) = \frac{d}{dt} C(t) + \gamma_s \quad (12)$$

208 and

$$\begin{aligned} \log I_r(t) &= C(t) + \mu_r + \int_0^t \gamma_s d\tau - \int_0^t u(\tau)\gamma_T d\tau - \int_0^t (1 - u(\tau))\gamma_U d\tau \\ &= C(t) + \mu_r + \int_0^t \gamma_s - u(\tau)(\gamma_T - \gamma_U) - \gamma_U d\tau \\ &= C(t) + \mu_r + (\gamma_s - \gamma_U)t - (\gamma_T - \gamma_U) \int_0^t u(\tau) d\tau \end{aligned} \quad (13)$$

209 Once again we follow the same reasoning for the resistant trajectory intercept μ_r , relating it to I_{r0} as:

$$\mu_r = \log I_{r0} - C(0) \quad (14)$$

210 Note that $\frac{d}{dt}C(t)$ exists as long as the associated covariance kernel is sufficiently smooth such as in the
 211 case of the radial basis function (RBF) kernel [33] which we used. Evaluating a full-rank, Gaussian
 212 process with differentiable trajectories on the entirety of the mesh would be prohibitively expensive
 213 due to the $O(n^3)$ computational complexity, where n is the number of grid points. Such a high
 214 computational cost would make the model infeasible. Instead, we work with a low-rank representation
 215 of $C(t)$ based on the framework introduced in [34]. This leads to the representation of the low-rank
 216 projection of $C(t)$, denoted by $\hat{C}(t)$

$$\hat{C}(t) = \sum_{j=1}^m S_{\text{RBF}} \left(\sqrt{\frac{j\pi}{2L}}; \rho, \alpha \right) \sqrt{\frac{1}{L}} \sin \left(\frac{j\pi}{2L}(t+L) \right) f_j \quad (15)$$

217 and

$$\frac{d}{dt} \hat{C}(t) = \sum_{j=1}^m S_{\text{RBF}} \left(\sqrt{\frac{j\pi}{2L}}; \rho, \alpha \right) \sqrt{\frac{1}{L}} \frac{j\pi}{2L} \cos \left(\frac{j\pi}{2L}(t+L) \right) f_j \quad (16)$$

218 This reduces the evaluation complexity of the Gaussian process prior from $O(n^3)$ to $O(nm)$. L and
 219 m are approximation parameters that need to be specified a-priori, see [34] for details. In practice we
 220 used the Hilbert Space Gaussian Process (HSGP) approximation with parameters $L = 6.5$ and $m = 60$.
 221 These approximation parameters are appropriate for the 99% interval of the length-scale prior used
 222 as per [34]. Where f_j are independent and identically distributed random variables following the
 223 standard Gaussian distribution, $S_{\text{RBF}}(\cdot; \cdot, \cdot)$ is the appropriate spectral density for the RBF kernel, ρ
 224 is the kernel length scale and α is the marginal standard deviation of the kernel [34].

225 Denote by $\boldsymbol{\theta} = (\gamma_s, \gamma_U, \gamma_T, I_{s0}, I_{r0}, \hat{C}(t))$ the parameters of the pathogen dynamics model. We can now
 226 factorise the model posterior $\pi(\boldsymbol{\theta}, \alpha, \rho, f_{1:m} | \mathbf{g}_s, \mathbf{g}_r)$, suppressing dependency on t where appropriate:

$$\pi(\boldsymbol{\theta}, \alpha, \rho, f_{1:m} | \mathbf{g}_s, \mathbf{g}_r) \propto \pi(\mathbf{g}_s | \lambda_s) \pi(\mathbf{g}_r | \lambda_r) \pi(\lambda_s | \boldsymbol{\theta}) \pi(\lambda_r | \boldsymbol{\theta}) \pi(\boldsymbol{\theta}, \alpha, \rho, f_{1:m}) \quad (17)$$

227 The first two terms are computed using the coalescent likelihood in Equation 7. The third term is
 228 given by combining Equations 6, 10 and 12. The fourth term is obtained by combining Equations 6,
 229 12 and 13. Finally, the last term is given by:

$$\pi(\boldsymbol{\theta}, \alpha, \rho, f_{1:m}) = \pi(\hat{C}(t) | \alpha, \rho, f_{1:m}) \pi(\gamma_T | \gamma_s) \pi(\gamma_U | \gamma_s) \pi(\gamma_s) \pi(I_{s0}) \pi(I_{r0}) \pi(\alpha) \pi(\rho) \pi(f_{1:m}) \quad (18)$$

230 where the first term is given by the Gaussian process (Equations 15 and 16) and the remaining terms
 231 correspond to the prior distributions listed below.

232 **Choice of prior and parameterisation**

Parameter	Symbol	Prior
Susceptible lineage recovery rate	γ_s	<code>log-normal(log γ^*, σ)</code>
Resistant lineage recovery rate if treated with focal antibiotic	γ_T	<code>normal(γ_s, $0.3\gamma^*$) \mathbb{1}[x > 0]</code>
Resistant lineage recovery rate if treated with other antibiotic	γ_U	<code>normal(γ_s, $0.3\gamma^*$) \mathbb{1}[x > 0]</code>
Initial prevalence of sensitive lineage	I_{s0}	<code>log-normal(6, 2)</code>
Initial prevalence of resistant lineage	I_{r0}	<code>log-normal(6, 2)</code>
GP kernel marginal variance	α	<code>gamma(4, 4)</code>
GP kernel length scale	ρ	<code>inverse-gamma(4.63, 2.21)</code>
Approximate GP functions	$f_{1:m}$	<code>N(0, 1)</code>

Table 1: Summary of the parameters and priors used in the model.

233 The model is parameterised with the priors summarised in Table 1. The data is not expected to be
 234 very informative about the value of γ_s . As such, we impose a fairly informative prior on this parameter,
 235 centred around a guess γ^* which must be known and supplied *a priori*. σ then governs how informative
 236 the prior is. We typically use a value of $\sigma = 0.3$, which includes relative fluctuations of over 50% in its
 237 95% interval. The higher the value of σ , the more complicated the geometry and subsequently sampling
 238 of the posterior becomes. γ_T and γ_U represent the recovery rates for the resistant lineage when the
 239 resistant lineage is treated with the focal antibiotic of interest, or another antibiotic, respectively. A
 240 normal distribution centred at γ_s and truncated to positive values only is a natural choice. We choose
 241 its standard deviation to be $0.3\gamma^*$ as this puts $> 99\%$ of the weight within $2\gamma^*$ thus making implausibly
 242 large fluctuations unlikely. Such large fluctuations are hardly of interest here since they would lead to
 243 a very rapid selective sweep or extinction. The recovery rates γ_T and γ_U are related to the absolute
 244 changes in recovery and therefore fitness parameters using Equation 5. $\gamma_U > \gamma_s$ corresponds to faster
 245 recovery when the resistant lineage is treated with an antimicrobial it is sensitive to and therefore
 246 a cost of resistance. $\gamma_T < \gamma_s$ corresponds to slower recovery when the resistant lineage is treated
 247 with the antimicrobial of interest and therefore a benefit of resistance. If instead a large proportion
 248 of posterior probability mass has $\gamma_U < \gamma_s$ or $\gamma_T > \gamma_s$, we conclude that the result is consistent with
 249 either the cost or the benefit of resistance not being significantly present. The prior on ρ was chosen so
 250 that approximately 1% of mass lies on values of $\rho < 0.2$ and approximately 1% of mass lies on $\rho > 2$.
 251 The lower bound was chosen to avoid over-fitting, and the upper bound to suppress length scales that
 252 exceed the range of data and thus cannot be informed about by the data.

253 In practice, due to our choice of a sampling approach we need to parametrise γ_U and γ_T on an
 254 unconstrained space, and ideally also weaken the dependency on γ_s . To do so we introduce parameters
 255 \tilde{q}_U and \tilde{q}_T , and define γ_U and γ_T to be a deterministic transformation of these

$$\begin{aligned}\gamma_U &= \log(1 + \exp \{\tilde{q}_U + \log \gamma_s\}) \\ \gamma_T &= \log(1 + \exp \{\tilde{q}_T + \log \gamma_s\})\end{aligned}\tag{19}$$

256 The Jacobian adjustment to the likelihood associated with this transformation is proportional to

$$|\det J_q| \propto (1 + \exp \{-\tilde{q}_T - \log \gamma_s\})^{-1} (1 + \exp \{-\tilde{q}_U - \log \gamma_s\})^{-1}\tag{20}$$

257 Computational implementation

258 The posterior in Equation 17 is a high dimensional distribution and we expect many parameters to
259 have a high degree of interdependency. In order to sample from this distribution, we use Dynamic
260 Hamiltonian Monte Carlo, a Hamiltonian Monte Carlo (HMC) sampler available in Stan [35]. HMC is a
261 Markov chain Monte Carlo approach that due to possessing energy conserving properties is able to take
262 large steps between individual states while maintaining a high acceptance rates. This makes it efficient
263 at sampling from moderately high dimensional posterior distributions with differentiable likelihoods,
264 while requiring a much lower number of iterations. We implemented the model and inference method in
265 a R package which is available at <https://github.com/dhelekal/ResistPhy/>. All results shown used
266 4 chains with 2000 iterations for warmup and 2000 iterations for sampling. For all model parameters
267 and all analysis the bulk effective sample size (bulk-ESS) was always greater than 500, and all \hat{R}
268 statistics were lower than 1.05 [36], values that indicate no issues with mixing. We also checked that
269 there were no divergent transitions at least during the sampling phase.

270 Use of simulated and real datasets

271 For all simulations we use a stochastic, discrete state-space version of the multi-lineage SIS in Equation
272 1. The system is simulated using tau-leaping [37]. More specifically we consider a scenario with three
273 lineages simulated over the course of 19 years. Two lineages are set to be susceptible and thus unaffected
274 by antibiotic usage fluctuations and one is set to be resistant. The first lineage aims to represent the
275 unobserved bulk of the population and thus is set to start at much higher prevalence. Conditional on
276 the trajectories of the two lineages, we sample phylogenies under Kingman's coalescent with varying
277 effective population size $N_e(t)$ following Equation 6 conditional on the trajectories [28]. The parameters
278 for the simulation were selected as to consistently provide a reasonable range of plausible behaviours
279 so that resistant lineages would reach prevalence with orders of magnitude between 10^2 to 10^4 .

280 A total of 1102 genomes were collected between 2000 and 2013 by the CDC Gonococcal Isolate
281 Surveillance (GISP) Project [38]. A maximum-likelihood phylogeny was computed using PhyML [39],
282 which was corrected for recombination using ClonalFrameML [40] and dated using BactDating [24].
283 This dated phylogeny is the same as previously used in an analysis of hidden population structure
284 [41]. The distribution of primary antimicrobial drugs used to treat gonorrhoea among participants
285 of the GISP project between 1988 and 2019 was obtained from the GISP reports available at
286 <https://www.cdc.gov/std/statistics/archive.htm>. Note that usage of ciprofloxacin and ofloxacin
287 were combined into a single fluoroquinolone category. All the data and code used in the simulated and
288 real datasets analyses is available at <https://github.com/dhelekal/ResistPhy/tree/main/run>.

289 RESULTS

290 Detailed analysis of a single simulated dataset

291 To validate the performance of this model we first resort to simulation from a 3-lineages stochastic
292 SIS with population size $N(t)$, transmission rate $\beta(t)$ and antimicrobial usage function $u(t)$ varying
293 over the past 20 years, as illustrated in Figure 1. The first two lineages are susceptible and thus
294 unaffected by fluctuations in antimicrobial usage, whereas the third lineage is resistant and therefore

295 affected. The first lineage represents the bulk of the susceptible lineages and is thus left unobserved.
296 The remaining two lineages represent the observed lineages, susceptible and resistant, respectively.
297 The per-day recovery rate of the sensitive lineage was set to $\gamma_s = 1/60$, the fitness cost of resistance to
298 $q_U = 1.25$ and the fitness benefit of resistance to $q_T = -2.7$. From each of these two observed lineages,
299 a dated phylogeny with 200 leaves was simulated. The sampling dates were randomly assigned to
300 one of the first six years, with the relative probability of a particular year being chosen proportional
301 to the total prevalence in that year. We performed inference on this simulated dataset; the traces
302 are shown in Figure S1 and the posterior distribution of the kernel parameters in Figure S2. The
303 prevalence and reproduction number $R(t)$ of both the susceptible and resistant lineages are shown in
304 Figure 2. As expected, the inferred values followed the correct values used in the simulation. The
305 inferred values of the susceptible lineage recovery rate γ_s and the cost and benefit of resistance q_U and
306 q_T were also found to be close to their correct values, as shown in Figure 3. The posterior distribution
307 of γ_s was almost identical to the prior, which was centered on the correct value 1/60, reflecting the
308 fact that the data is uninformative about this parameter and stressing the importance of using an
309 informative prior. There was a strong negative correlation between the inferred values of q_U and q_T ,
310 as expected since these two parameters play opposite roles in the overall fitness of the resistant lineage
311 relative to the sensitive lineage. Nevertheless, we detected both the cost and the benefit associated
312 with resistance, since the ranges of inferred values for q_U and q_T were respectively above and below
313 one, contrary to their log-normal priors with mean one (Figure 3). Finally, we computed the posterior
314 predictive distribution [42] for the number of ancestral lineages through time $A(t)$ and compared this
315 with the input phylogenetic data (Figure S3). The data and posterior predictive trajectories were
316 similar, indicating a good fit of the model to the data as indeed would be expected here since the same
317 model was used for simulation and inference.

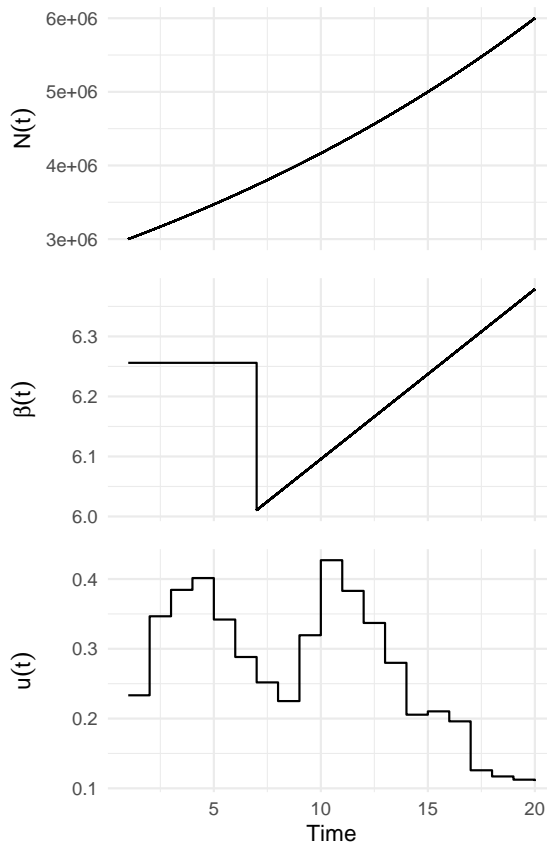


Figure 1: Host population size function $N(t)$, transmission rate over time $\beta(t)$ and antibiotic usage function $u(t)$ used in the simulated datasets.

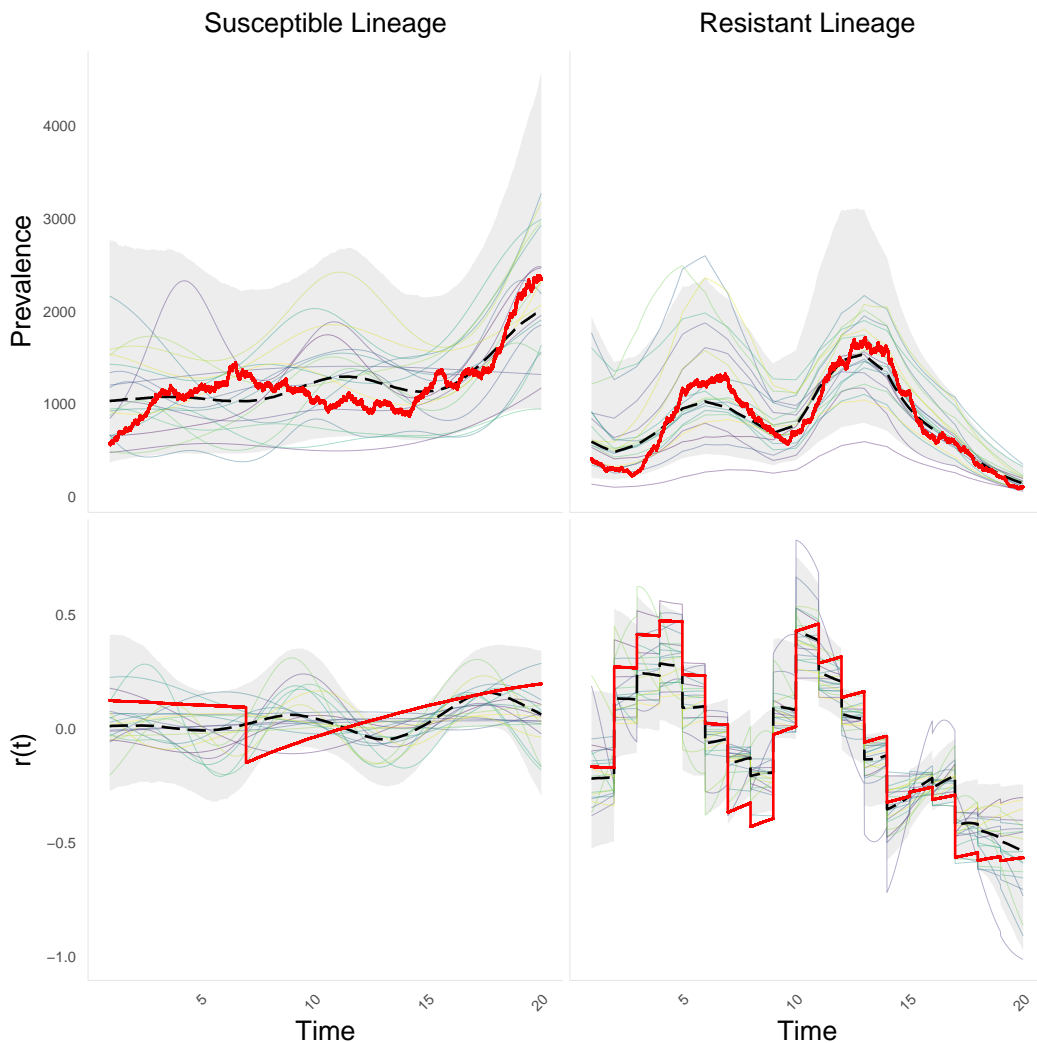


Figure 2: Posterior summary of dynamics for the sensitive (left) and resistant (right) lineages, showing prevalence (top) and reproduction number (bottom). Bold solid red lines indicates simulated values. Posterior median in bold dashed black line. Shaded bands indicate 95% posterior credible intervals. Solid light lines represent posterior draws.

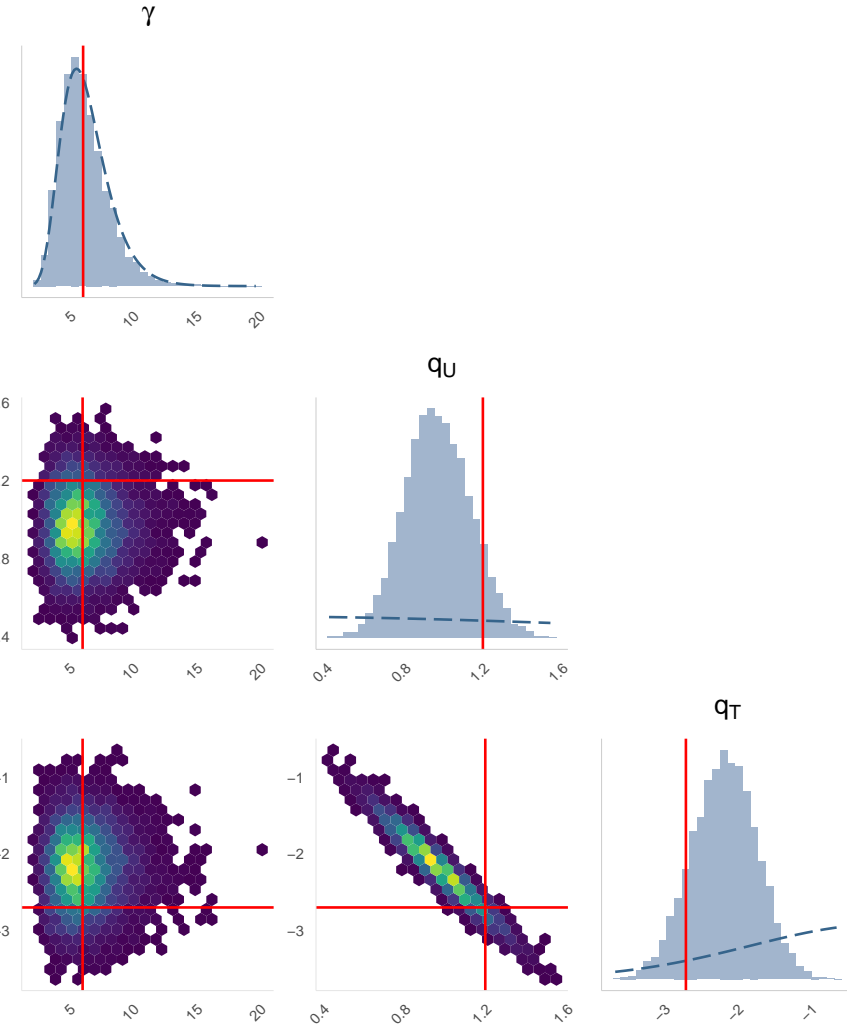


Figure 3: Marginal and joint posterior distributions for the recovery rate of the sensitive lineage (γ_s), fitness cost (q_U) and fitness benefit (q_T) of resistance. Bold red solid lines indicate simulation values. Bold blue dashed lines indicate prior density values.

318 **Benchmark using multiple simulated datasets**

319 We repeated the same application of our inference method to data simulated in the same conditions
 320 as described above and illustrated in Figure 1, except the values of the fitness cost and benefit of
 321 resistance were varied. A total of 50 simulated datasets were generated and analysed, with the fitness
 322 cost q_U increasing linearly from 1 to 1.2, and the fitness benefit q_T decreasing linearly from 1 to 0.5.
 323 The prevalence of the susceptible and resistant lineages in these simulations are shown in Figure S4.
 324 The results of inference are illustrated in Figure 4 and show that in almost all cases the posterior 95%
 325 credible intervals covered the correct values of the fitness cost and benefit of resistance used in the
 326 simulations.

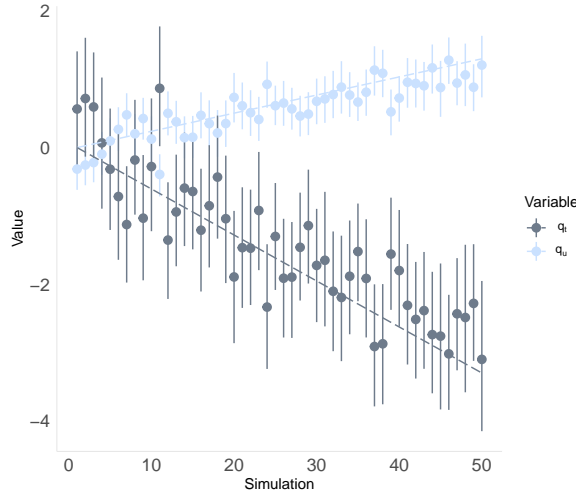


Figure 4: Inferred parameters versus correct values. A total of 50 simulated datasets were generated, with decreasing values of q_T and increasing values of q_U as shown by the dotted lines in grey and blue, respectively. For each simulated dataset we applied our inference method. The grey and blue dots show the mean inferred values of q_T and q_U , respectively, with vertical bars representing the 95% credible intervals for both parameters.

327 Application to fluoroquinolone resistant *N. gonorrhoeae* in USA

328 We demonstrate the use of our model and inferential framework by estimating the cost and benefit
 329 of fluoroquinolone resistance in *N. gonorrhoeae*. Based on the 1102 genomes collected between 2000
 330 and 2013 by the CDC Gonococcal Isolate Surveillance Project [38], a recombination-corrected tree
 331 was constructed using ClonalFrameML [40] and dated using BactDating [24]. As there are two major
 332 fluoroquinolone resistant lineages present in this phylogeny [38], we decided to do a comparative study.
 333 The two fluoroquinolone resistant lineages and one fluoroquinolone susceptible lineage were selected
 334 based on similar resistance profiles against other relevant antibiotics. By inspecting the antibiotic usage
 335 data and the resistance profiles for the the three lineages (Figure 5) we can see that the resistance
 336 profiles match for antimicrobials that were in use as primary treatment at significant levels after 1995.
 337 As such this is the year we set as the analysis start date ($t_{\min} = 1995$) and the end date is the date
 338 when the last genomes were collected ($t_{\max} = 2013$). Note that a subclade within the susceptible
 339 lineage that displayed a *de novo* gain of resistance to cefixime has been removed. The prior mean for
 340 the per-day recovery rate for the susceptible lineage was set to $\gamma^* = 1/90$ based on previous gonorrhoea
 341 modelling studies [10, 43, 44].

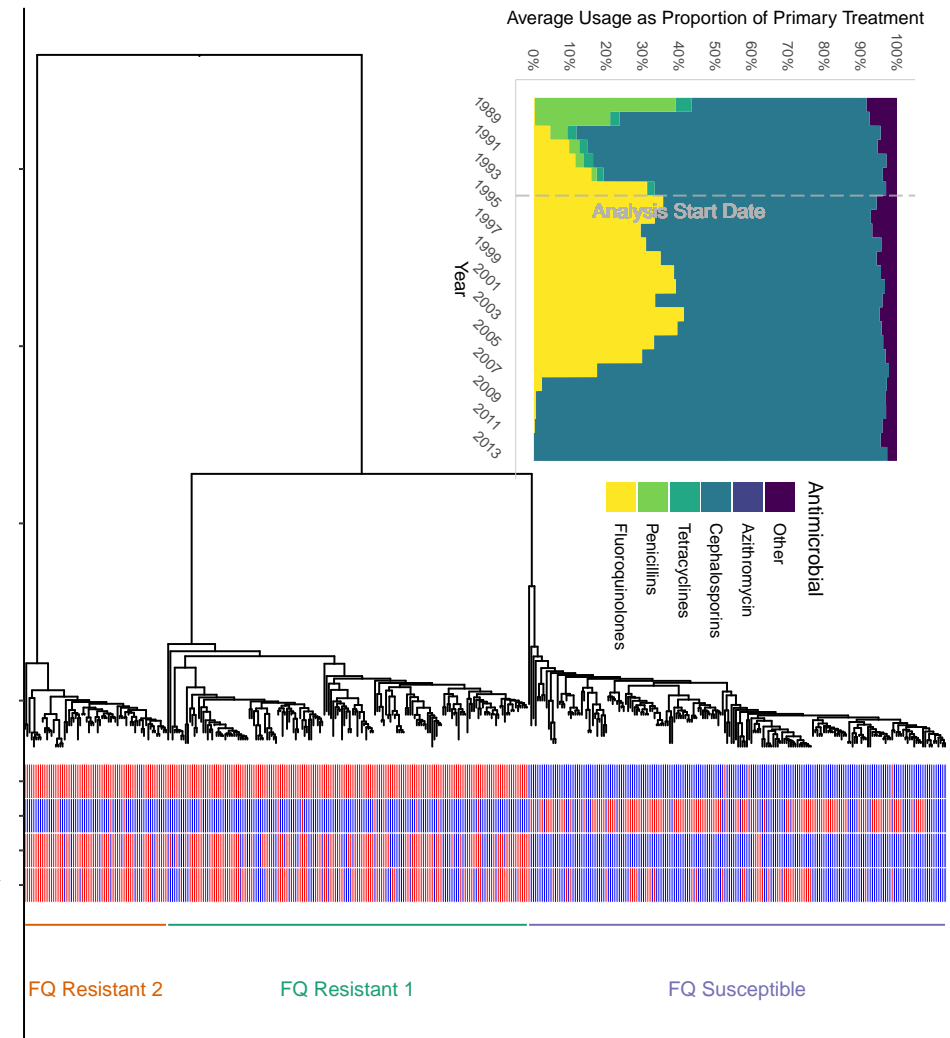


Figure 5: Antibiotic usage data and phylogeny used for the application to fluoroquinolone resistant *N. gonorrhoeae*.

We performed inference for this dataset; the traces are shown in Figure S5 and the posterior distribution of kernel parameters in Figure S6. Figure 6 depicts the summary of posterior latent transmission dynamics for the two resistant lineages, whereas Figure S7 shows the same for the susceptible lineage. The two resistant lineages have similar dynamics, with a peak in prevalence around 2007, which corresponds to the moment when fluoroquinolone use dropped (Figure 5). Figure 7 depicts the marginal and joint posterior distributions for the resistance parameters q_U and q_T for both resistant lineages. This is consistent with there being both a cost and benefit to fluoroquinolone resistance for both lineages, since both q_U and q_T are respectively localised below 1 and above 1, with high posterior probability. It is noteworthy that while both of these lineages come from distinct genetic background, their resistance profile is qualitatively very similar, indicating both of these lineages faced similar selective pressures and neither seems to have successfully adapted to overcome the fitness cost associated with fluoroquinolone resistance. We used a posterior predictive approach to ensure that the model can explain the data appropriately [42]. Posterior predictive trajectories for the function of

355 ancestral lineages through time $A(t)$ were simulated and found to be very similar to the ones implied
356 by the phylogenetic data (Figure S8).

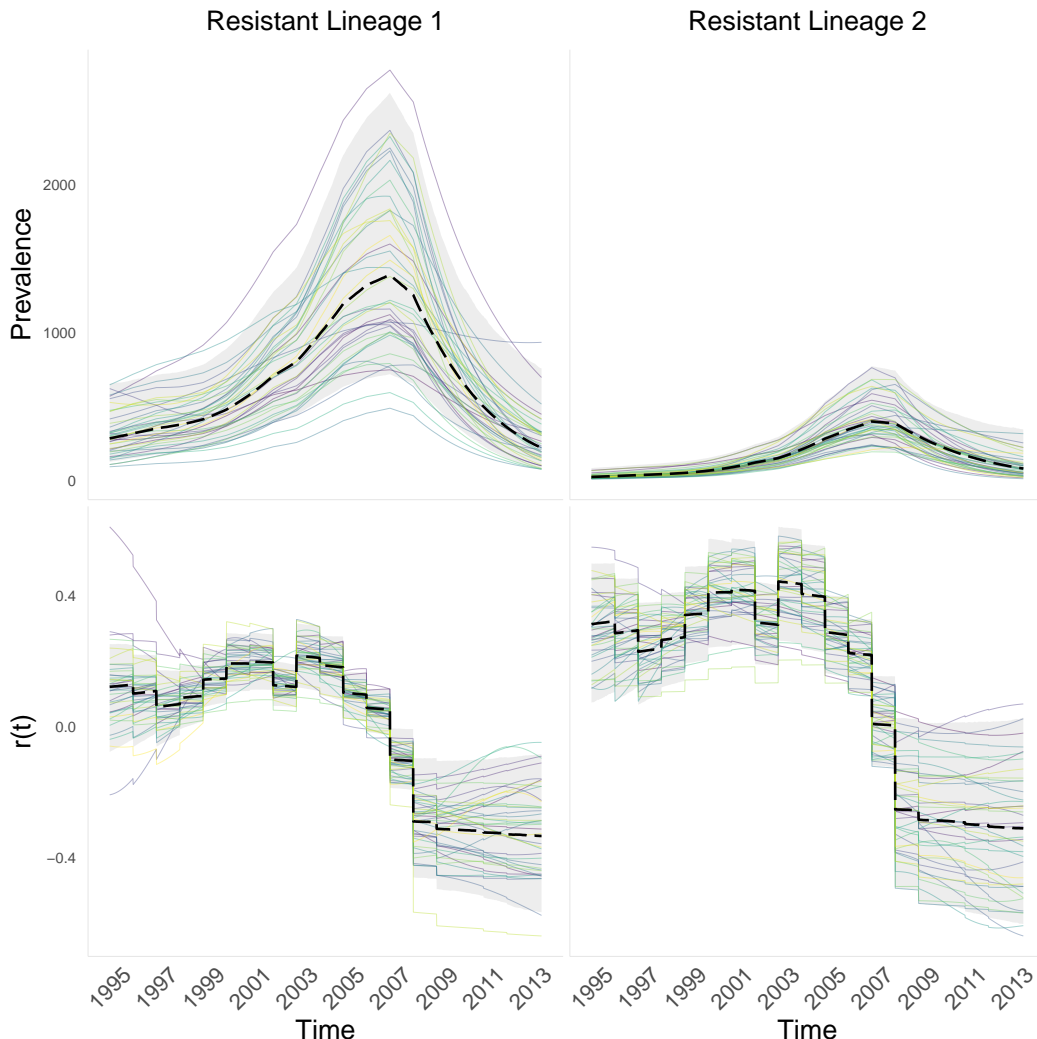


Figure 6: Posterior epidemic dynamics for both fluoroquinolone resistant lineages of *N. gonorrhoeae*.

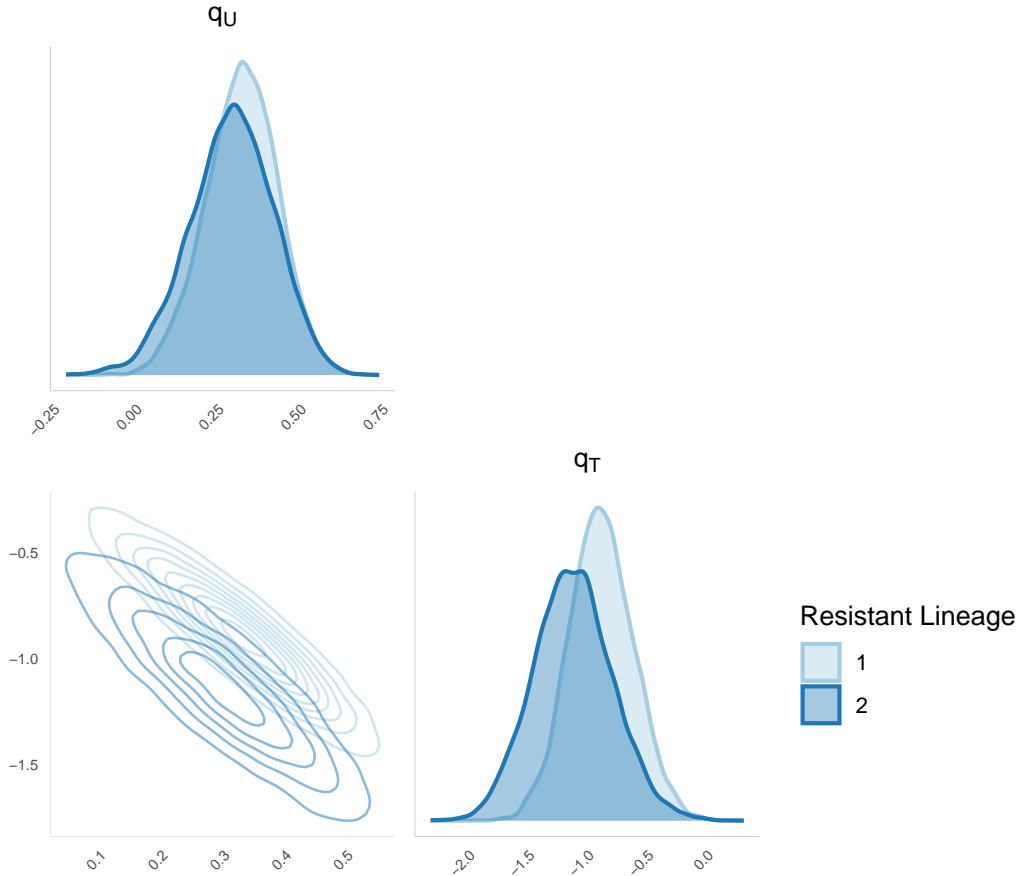


Figure 7: Marginal and joint posterior distribution for the cost (q_U) and benefit (q_T) of both fluoroquinolone resistant lineages of *N. gonorrhoeae*.

357 Under the assumption of perfect competition between lineages, if we want to ensure that a resistant
 358 lineage cannot establish, and its proportion decays sufficiently fast, we fix a decay factor $c > 0$ and aim
 359 to ensure that the growth rate of the resistant lineage is c units lower than that of the sensitive lineage,
 360 that is $r_s(t) - r_r(t) > c$. Note that $r(t)$ is the growth rate through time, not $R(t)$, the time varying
 361 reproduction number. We choose to work with growth rates as these are less sensitive to susceptible
 362 recovery rate mispecification. Given that the lineages have the same transmission rate function $b(t)$,
 363 this condition is equivalent to $\gamma_s(t) - \gamma_r(t) > c$, and using the definition of $\gamma_r(t)$ from Equation 3,
 364 this is equivalent to $u(t)q_T + (1 - u(t))q_U > c$. We use this to estimate posterior probabilities the
 365 differences in growth rates between the susceptible lineage and each of both resistant lineages exceed
 366 c as shown in Figure 8. In order to be 95% certain that the resistant lineages remain at a lower fitness
 367 than the susceptible lineage, fluoroquinolone should not be prescribed to more than $\sim 20\%$ and $\sim 15\%$
 368 of infected individuals, for resistant lineages 1 and 2, respectively.

Posterior Probability of $r_s(t) - r_r(t) > c$ given usage level

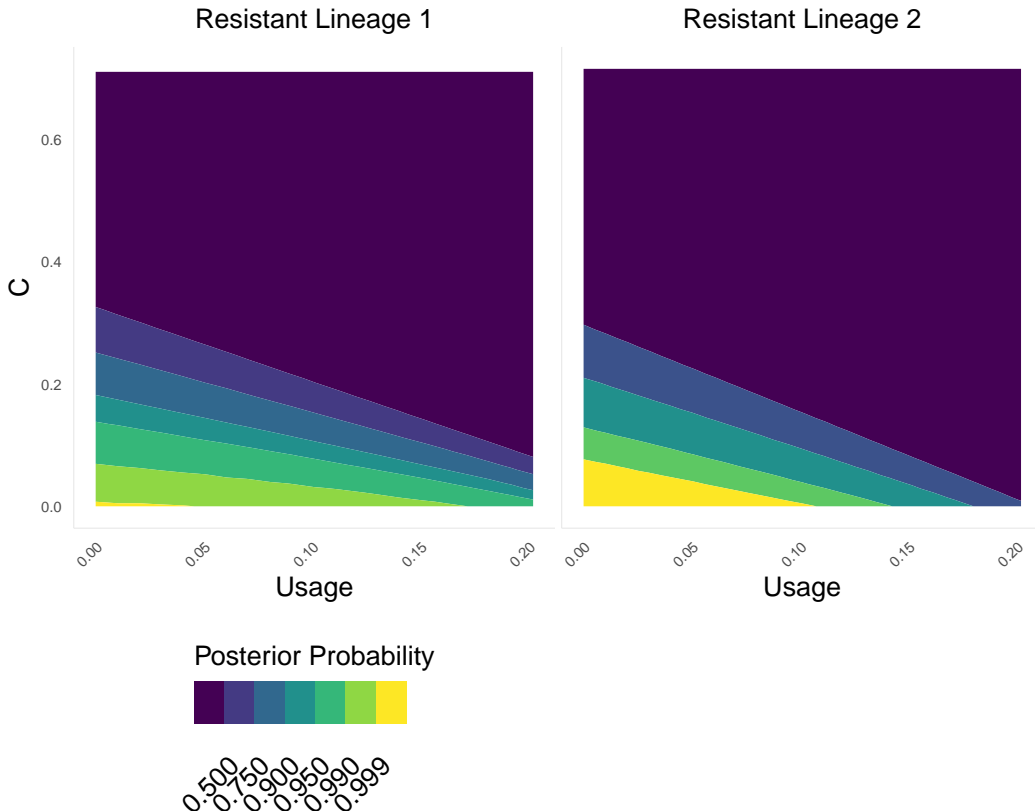


Figure 8: Posterior probabilities of $R_r(t)/R_s(t) < C$ given usage $u(t)$ in the x-axis and value of C in the y-axis, for both fluoroquinolone resistant lineages of *N. gonorrhoeae*.

369 **DISCUSSION**

370 A bacterial pathogen lineage that is resistant to a given antibiotic incurs both a fitness cost and a fitness
371 benefit compared to similar susceptible lineages [8]. When the antibiotic is used extensively, the benefit
372 is likely to be greater than the cost. In that case, a resistant lineage has a selective advantage over
373 susceptible lineages, and therefore grows at a faster rate. Conversely, if the antibiotic is used rarely
374 or not at all, the benefit is likely to become smaller than the cost, which will lead to the resistant
375 lineage decreasing in frequency. Estimating these parameters is therefore of primary importance to
376 determine how antibiotics should be prescribed without causing an increase in resistance [9]. Here, we
377 have shown how genome sequencing data coupled with data on antibiotic prescriptions can be used for
378 this purpose, following on previous work that demonstrated the link between epidemic dynamics and

379 phylogenetics [13, 19, 20, 28]. By comparing the phylodynamic trajectories of susceptible and resistant
380 lineages, and relating them with a known function of antibiotic use, we show that it is possible to
381 estimate separately the parameters corresponding to the fitness cost and benefit of resistance. In
382 particular, we reanalysed a large published collection of *N. gonorrhoeae* genomes [38]. We were able
383 to infer these parameters for two lineages of *N. gonorrhoeae* resistant to fluoroquinolones, and found
384 similar estimates of cost and benefit in both (Figure 7). We were able to use this knowledge to make
385 recommendations on antibiotic stewardship of fluoroquinolones (Figure 8).

386 Dated phylogenies for both susceptible and resistant lineages are needed as input into our method.
387 Several software tools can be used to produce this either from a sequence alignment, for example
388 BEAST [22] and BEAST2 [23], or from an undated phylogeny, for example treedater [45] and
389 BactDating [24]. Building such a dated phylogeny requires either the population to be measurably
390 evolving over the sampling period [46, 47], or a previous estimate of the molecular clock rate [48].
391 Another input required by our method is the antibiotic usage function over a relevant timeframe and
392 geographical location. This may not always be available in all historical contexts, but efforts are
393 increasingly being made to capture this data [49]. Finally, our method requires an informative prior
394 of the recovery rate for the susceptible lineage (see Table 1), since this is typically not identifiable
395 from the data, as in many similar compartmental epidemic models [50]. This prior needs to be chosen
396 carefully depending on the infectious disease under study and based on the existing scientific literature.

397 Our inferential methodology is based on a well-defined and relatively simple epidemic model (Equation
398 4) which means making a number of assumptions the validity of which was considered before performing
399 our analysis. Our model assumes multiple-lineage pathogen dynamics driven by person-to-person
400 transmission in a well mixed host population in the absence of any significant population structure, so
401 that there is perfect competition between lineages. It also assumes that individuals become infectious
402 as soon as they are infected, that their infectiousness remains constant until they recover, after which
403 they become susceptible again without any immunity being gained. This list of relatively strong
404 assumptions may seem to preclude application to any real infectious disease, but they are necessary
405 to obtain a model under which inference can be performed. Furthermore, violation of some of these
406 assumptions does not necessarily invalidate the results of inference. For example, if infection causes
407 immunity, this will effectively reduce the number $S(t)$ of susceptible individuals (Equation 2), but this
408 number is not assumed to be constant in our model. In fact both the size $N(t)$ of the host population
409 and the number $S(t)$ of susceptible individuals are integrated out as part of our parameterisation
410 in terms of the function $b(t)$ (cf Equation 4), so the inference is robust as long as the immunity
411 conferred applies to all lineages under study. Likewise the assumption of an unstructured population
412 may seem problematic, including in our application to *N. gonorrhoeae* throughout the USA, but for
413 anything other than small local outbreaks the genomes available for analysis are sparsely sampled from
414 the whole infected population [51]. In these conditions, any effect of the host population structure
415 on phylodynamics is likely to be insignificant as long as an effective rather than actual number of
416 infections is considered [52, 53].

417 The compatibility of our model with the phylogenetic data under analysis can be tested using posterior
418 predictive distribution checks (Figures S3 and S8). If these tests fail, or if the model assumptions are
419 thought to be inappropriate, a solution may be to resort to other methods that postprocess a dated
420 phylogeny [25] but make less assumptions, at the cost of not inferring directly the parameters of
421 resistance. Alternative approaches includes non-parametric methods that detect differences in the
422 branching patterns in different lineages [41, 54] as well as methods parameterised in terms of the
423 pathogen population size growth rather than underlying epidemiological drivers [15, 55]. However, our
424 model-based approach is both general and flexible, so that we expect it to be applicable in many settings
425 using our software implementation which is available at <https://github.com/dhelekal/ResistPhy/>.
426 We believe that this methodology, applied to the increasingly large genomic databases on many

427 bacterial pathogens, will help quantify the exact link between antibiotic usage and resistance and
428 therefore provide a much-needed evidence basis for the design of future antibiotic prescription strategies
429 [9, 56, 57].

430 ACKNOWLEDGMENTS

431 We acknowledge funding from the National Institute for Health Research (NIHR) Health Protection
432 Research Unit in Genomics and Enabling Data. This work was supported by the UK Engineering and
433 Physical Sciences Research Council (EPSRC) grant EP/S022244/1 for the EPSRC Centre for Doctoral
434 Training in Mathematics for Real-World Systems II.

435 REFERENCES

436 [1] CDC, 2013 Antibiotic resistance threats in the United States, 2013. *Current* p. 114. ISSN
437 10985530. (doi:CS239559-B).

438 [2] O'Neill, J., 2016 *Tackling drug-resistant infections globally: final report and recommendations*.
439 London: Wellcome Trust \& HM Government.

440 [3] Murray, C. J., Ikuta, K. S., Sharara, F., Swetschinski, L., Aguilar, G. R., Gray, A., Han, C.,
441 Bisignano, C., Rao, P., Wool, E. *et al.*, 2022 Global burden of bacterial antimicrobial resistance
442 in 2019: a systematic analysis. *The Lancet* **399**, 629–655.

443 [4] Clatworthy, A. E., Pierson, E. & Hung, D. T., 2007 Targeting virulence: a new paradigm for
444 antimicrobial therapy. *Nat. Chem. Biol.* **3**, 541–548. ISSN 1552-4450. (doi:10.1038/nchembio.
445 2007.24).

446 [5] Bonhoeffer, S., Lipsitch, M. & Levin, B. R., 1997 Evaluating treatment protocols to prevent
447 antibiotic resistance. *Proc Natl Acad Sci U S A* **94**, 12106–12111. ISSN 0027-8424 (Print).
448 (doi:10.1073/pnas.94.22.12106).

449 [6] Austin, D. J., Kristinsson, K. G. & Anderson, R. M., 1999 The relationship between the volume
450 of antimicrobial consumption in human communities and the frequency of resistance. *PNAS* **96**,
451 1152–1156. ISSN 0027-8424. (doi:10.1073/pnas.96.3.1152).

452 [7] Spicknall, I. H., Foxman, B., Marrs, C. F. & Eisenberg, J. N. S., 2013 A modeling framework
453 for the evolution and spread of antibiotic resistance: Literature review and model categorization.
454 *Am. J. Epidemiol.* **178**, 508–520. ISSN 00029262. (doi:10.1093/aje/kwt017).

455 [8] Andersson, D. I. & Levin, B. R., 1999 The biological cost of antibiotic resistance. *Curr. Opin.
456 Microbiol.* **2**, 489–493. ISSN 13695274. (doi:10.1016/S1369-5274(99)00005-3).

457 [9] Andersson, D. I. & Hughes, D., 2010 Antibiotic resistance and its cost: is it possible to reverse
458 resistance? *Nat. Rev. Microbiol.* **8**, 260–271. ISSN 1740-1526. (doi:10.1038/nrmicro2319).

459 [10] Whittles, L. K., White, P. J. & Didelot, X., 2017 Estimating the fitness benefit and cost of cefixime
460 resistance in *Neisseria gonorrhoeae* to inform prescription policy: A modelling study. *PLoS Med.*
461 **14**, e1002416. (doi:10.1371/journal.pmed.1002416).

462 [11] Rubin, D. H., Ma, K. C., Westervelt, K. A., Hullahalli, K., Waldor, M. K. & Grad, Y. H.,
463 2022 Variation in supplemental carbon dioxide requirements defines lineage-specific antibiotic
464 resistance acquisition in neisseria gonorrhoeae.
465 *bioRxiv* (doi:10.1101/2022.02.24.481660). Publisher: Cold Spring Harbor Laboratory preprint:
466 <https://www.biorxiv.org/content/early/2022/02/25/2022.02.24.481660.full.pdf>.

467 [12] Lehtinen, S., Blanquart, F., Lipsitch, M., Fraser, C. & Collaboration, w. t. M. P., 2019 On the
468 evolutionary ecology of multidrug resistance in bacteria. *PLOS Pathogens* **15**, e1007763. ISSN
469 1553-7374. (doi:10.1371/journal.ppat.1007763). Publisher: Public Library of Science.

470 [13] Pybus, O. G. & Rambaut, A., 2009 Evolutionary analysis of the dynamics of viral infectious
471 disease. *Nat. Rev. Genet.* **10**, 540–50. ISSN 1471-0064. (doi:10.1038/nrg2583).

472 [14] Volz, E. M. & Frost, S. D. W., 2014 Sampling through time and phylodynamic inference with
473 coalescent and birth – death models. *J. R. Soc. Interface* **11**, 20140945.

474 [15] Volz, E. M. & Didelot, X., 2018 Modeling the Growth and Decline of Pathogen Effective Population
475 Size Provides Insight into Epidemic Dynamics and Drivers of Antimicrobial Resistance. *Syst. Biol.*
476 **67**, 719–728. ISSN 1063-5157. (doi:10.1093/sysbio/syy007).

477 [16] Kühnert, D., Kouyos, R., Shirreff, G., Pečerska, J., Scherrer, A. U., Böni, J., Yerly, S., Klimkait,
478 T., Aubert, V., Günthard, H. F. *et al.*, 2018 Quantifying the fitness cost of HIV-1 drug resistance
479 mutations through phylodynamics. *PLOS Pathogens* **14**, e1006895. ISSN 1553-7374. (doi:
480 10.1371/journal.ppat.1006895). Publisher: Public Library of Science.

481 [17] Pečerska, J., Kühnert, D., Meehan, C. J., Coscollá, M., de Jong, B. C., Gagneux, S. & Stadler,
482 T., 2021 Quantifying transmission fitness costs of multi-drug resistant tuberculosis. *Epidemics*
483 **36**, 100471. ISSN 1755-4365. (doi:10.1016/j.epidem.2021.100471).

484 [18] Ho, S. Y. W. & Shapiro, B., 2011 Skyline-plot methods for estimating demographic history
485 from nucleotide sequences. *Molecular Ecology Resources* **11**, 423–434. ISSN 1755098X. (doi:
486 10.1111/j.1755-0998.2011.02988.x).

487 [19] Volz, E. M., Kosakovsky Pond, S. L., Ward, M. J., Leigh Brown, A. J. & Frost, S. D. W.,
488 2009 Phylodynamics of infectious disease epidemics. *Genetics* **183**, 1421–30. ISSN 1943-2631.
489 (doi:10.1534/genetics.109.106021).

490 [20] Dearlove, B. & Wilson, D., 2013 Coalescent inference for infectious disease: Meta-analysis of
491 hepatitis C. *Philosophical Transactions of the Royal Society B* **368**, 20120314.

492 [21] Didelot, X., Bowden, R., Wilson, D. J., Peto, T. E. A. & Crook, D. W., 2012 Transforming
493 clinical microbiology with bacterial genome sequencing. *Nature Reviews Genetics* **13**, 601–612.
494 ISSN 1471-0056. (doi:10.1038/nrg3226).

495 [22] Suchard, M. A., Lemey, P., Baele, G., Ayres, D. L., Drummond, A. J. & Rambaut, A., 2018
496 Bayesian phylogenetic and phylodynamic data integration using BEAST 1.10. *Virus Evol.* **4**,
497 vey016. ISSN 2057-1577. (doi:10.1093/ve/vey016).

498 [23] Bouckaert, R., Vaughan, T. G., Fourment, M., Gavryushkina, A., Heled, J., Denise, K., Maio,
499 N. D., Matschiner, M., Ogilvie, H., Plessis, L. *et al.*, 2019 BEAST 2.5 : An Advanced Software
500 Platform for Bayesian Evolutionary Analysis. *PLoS Comput. Biol.* **15**, e1006650.

501 [24] Didelot, X., Croucher, N. J., Bentley, S. D., Harris, S. R. & Wilson, D. J., 2018 Bayesian inference
502 of ancestral dates on bacterial phylogenetic trees. *Nucleic Acids Res.* **46**, e134–e134. ISSN 0305-
503 1048. (doi:10.1093/nar/gky783).

504 [25] Didelot, X. & Parkhill, J., 2022 A scalable analytical approach from bacterial genomes to
505 epidemiology. *Philosophical Transactions of the Royal Society B: Biological Sciences* **377**,
506 20210246. (doi:10.1098/rstb.2021.0246).

507 [26] Allen, L. J., Kirupaharan, N. & Wilson, S. M., 2004 SIS epidemic models with multiple pathogen
508 strains. *Journal of Difference Equations and Applications* **10**, 53–75.

509 [27] Keeling, M. J. & Rohani, P., 2008 *Modeling Infectious Diseases in Humans and Animals*. Princeton
510 University Press. ISBN 9780691116174.

511 [28] Volz, E. M., 2012 Complex population dynamics and the coalescent under neutrality. *Genetics*
512 **190**, 187–201. ISSN 1943-2631. (doi:10.1534/genetics.111.134627).

513 [29] Griffiths, R. & Tavaré, S., 1994 Sampling theory for neutral alleles in a varying environment.
514 *Philos. Trans. R. Soc. B* **344**, 403–410.

515 [30] Gill, M. S., Lemey, P., Faria, N. R., Rambaut, A., Shapiro, B. & Suchard, M. A., 2013 Improving
516 bayesian population dynamics inference: A coalescent-based model for multiple loci. *Mol. Biol.*
517 *Evol.* **30**, 713–724. ISSN 07374038. (doi:10.1093/molbev/mss265).

518 [31] Griffiths, R. C., 2003 The frequency spectrum of a mutation, and its age, in a general diffusion
519 model. *Theoretical Population Biology* **64**, 241–251. ISSN 0040-5809. (doi:10.1016/S0040-5809(03)
520 00075-3).

521 [32] Etheridge, A., Pfaffelhuber, P. & Wakolbinger, A., 2006 An approximate sampling formula under
522 genetic hitchhiking. *The Annals of Applied Probability* **16**, 685–729. ISSN 1050-5164, 2168-8737.
523 (doi:10.1214/105051606000000114). Publisher: Institute of Mathematical Statistics.

524 [33] Rasmussen, C. E., 2004 *Gaussian Processes in Machine Learning*, pp. 63–71. Berlin, Heidelberg:
525 Springer Berlin Heidelberg. ISBN 978-3-540-28650-9. (doi:10.1007/978-3-540-28650-9_4).

526 [34] Riutort-Mayol, G., Bürkner, P.-C., Andersen, M. R., Solin, A. & Vehtari, A., 2022 Practical
527 hilbert space approximate bayesian gaussian processes for probabilistic programming. *arXiv* (doi:
528 10.48550/arXiv.2004.11408).

529 [35] Carpenter, B., Gelman, A., Hoffman, M. D., Lee, D., Goodrich, B., Betancourt, M., Brubaker,
530 M. A., Guo, J., Li, P. & Riddell, A., 2017 Stan: A probabilistic programming language. *J. Stat.*
531 *Softw.* **76**. ISSN 15487660. (doi:10.18637/jss.v076.i01).

532 [36] Vehtari, A., Gelman, A., Simpson, D., Carpenter, B. & Burkner, P. C., 2021 Rank-Normalization,
533 Folding, and Localization: An Improved R hat for Assessing Convergence of MCMC. *Bayesian*
534 *Anal.* **16**, 667–718. ISSN 19316690. (doi:10.1214/20-BA1221).

535 [37] Gillespie, D. T., 2001 Approximate accelerated stochastic simulation of chemically reacting
536 systems. *The Journal of Chemical Physics* **115**, 1716–1733. ISSN 0021-9606. (doi:10.1063/1.
537 1378322). Publisher: American Institute of Physics.

538 [38] Grad, Y. H., Harris, S. R., Kirkcaldy, R. D., Green, A. G., Marks, D. S., Bentley, S. D., Trees, D.,
539 Lipsitch, M., Diseases, I., Health, P. *et al.*, 2016 Genomic epidemiology of gonococcal resistance
540 to extended spectrum cephalosporins, macrolides, and fluoroquinolones in the US, 2000–2013. *J.*
541 *Infect. Dis.* **214**, 1579–1587. ISSN 0022-1899. (doi:10.1093/infdis/jiw420).

542 [39] Guindon, S., Dufayard, J.-F., Lefort, V., Anisimova, M., Hordijk, W. & Gascuel, O., 2010 New
543 algorithms and methods to estimate maximum-likelihood phylogenies: Assessing the performance
544 of PhyML 3.0. *Systematic biology* **59**, 307–21. ISSN 1076-836X. (doi:10.1093/sysbio/syq010).

545 [40] Didelot, X. & Wilson, D. J., 2015 ClonalFrameML: Efficient Inference of Recombination in
546 Whole Bacterial Genomes. *PLoS Comput. Biol.* **11**, e1004041. ISSN 1553-7358. (doi:
547 10.1371/journal.pcbi.1004041).

548 [41] Volz, E. M., Wiuf, C., Grad, Y. H., Frost, S. D. W., Dennis, A. M. & Didelot, X., 2020
549 Identification of hidden population structure in time-scaled phylogenies. *Systematic Biology* **69**,
550 884–896. (doi:10.1093/sysbio/syaa009).

551 [42] Gelman, A., Meng, X. & Stern, H., 1996 Posterior predictive assessment of model fitness via
552 realized discrepancies. *Stat Sinica* **6**, 733–807.

553 [43] Fingerhuth, S. M., Bonhoeffer, S., Low, N. & Althaus, C. L., 2016 Antibiotic-Resistant Neisseria
554 gonorrhoeae Spread Faster with More Treatment, Not More Sexual Partners. *PLOS Pathog.* **12**,
555 e1005611. ISSN 1553-7374. (doi:10.1371/journal.ppat.1005611).

556 [44] Whittles, L. K., White, P. J. & Didelot, X., 2019 A dynamic power-law sexual network
557 model of gonorrhoea outbreaks. *PLoS Comput. Biol.* **15**, e1006748. ISSN 1553-7358. (doi:
558 10.1371/journal.pcbi.1006748).

559 [45] Volz, E. M. & Frost, S. D. W., 2017 Scalable relaxed clock phylogenetic dating. *Virus Evolution*
560 **3**, vex025.

561 [46] Drummond, A. J., Pybus, O. G., Rambaut, A., Forsberg, R. & Rodrigo, A. G., 2003 Measurably
562 evolving populations. *Trends in Ecology and Evolution* **18**, 481–488. ISSN 01695347. (doi:
563 10.1016/S0169-5347(03)00216-7).

564 [47] Biek, R., Pybus, O. G., Lloyd-Smith, J. O. & Didelot, X., 2015 Measurably evolving pathogens
565 in the genomic era. *Trends in Ecology & Evolution* **30**, 306–313. ISSN 0169-5347. (doi:
566 10.1016/j.tree.2015.03.009).

567 [48] Duchêne, S., Holt, K. E., Weill, F.-X., Le Hello, S., Hawkey, J., Edwards, D. J., Fourment, M. &
568 Holmes, E. C., 2016 Genome-scale rates of evolutionary change in bacteria. *Microbial Genomics*
569 **2**, e000094. ISSN 2057-5858. (doi:10.1101/069492).

570 [49] Curtis, H. J. & Goldacre, B., 2018 Openprescribing: normalised data and software tool to research
571 trends in english nhs primary care prescribing 1998–2016. *BMJ open* **8**, e019921.

572 [50] Roosa, K. & Chowell, G., 2019 Assessing parameter identifiability in compartmental dynamic
573 models using a computational approach: application to infectious disease transmission models.
574 *Theoretical Biology and Medical Modelling* **16**, 1–15.

575 [51] Klinkenberg, D., Colijn, C. & Didelot, X., 2019 Methods for Outbreaks Using Genomic Data. In
576 *Handbook of Infectious Disease Data Analysis*, pp. 245–263. CRC Press.

577 [52] Nordborg, M., 1997 Structured coalescent processes on different time scales. *Genetics* **146**, 1501–
578 1514. ISSN 0016-6731.

579 [53] Frost, S. D. W. & Volz, E. M., 2010 Viral phylodynamics and the search for an 'effective number
580 of infections'. *Philosophical Transactions of the Royal Society B* **365**, 1879–1890. ISSN 0962-8436.
581 (doi:10.1098/rstb.2010.0060).

582 [54] Dearlove, B. L., Xiang, F. & Frost, S. D. W., 2017 Biased phylodynamic inferences from analysing
583 clusters of viral sequences. *Virus Evolution* **3**, 1–10. (doi:10.1093/ve/vex020).

584 [55] Helekal, D., Ledda, A., Volz, E., Wyllie, D. & Didelot, X., 2021 Bayesian inference of clonal
585 expansions in a dated phylogeny. *Systematic Biology* p. syab095. ISSN 1063-5157. (doi:
586 10.1093/sysbio/syab095).

587 [56] Michael, C. A., Dominey-Howes, D. & Labbate, M., 2014 The Antimicrobial Resistance Crisis:
588 Causes, Consequences, and Management. *Frontiers in Public Health* **2**. ISSN 2296-2565. (doi:
589 10.3389/fpubh.2014.00145).

590 [57] Holmes, A. H., Moore, L. S., Sundsfjord, A., Steinbakk, M., Regmi, S., Karkey, A., Guerin, P. J.
591 & Piddock, L. J., 2016 Understanding the mechanisms and drivers of antimicrobial resistance.
592 *Lancet* **387**, 176–187. ISSN 1474547X. (doi:10.1016/S0140-6736(15)00473-0).